

Optical study of the piezochromic transition in CuMoO_4 by pressure spectroscopy

F. Rodríguez* and D. Hernández

DCITIMAC, Facultad de Ciencias, Universidad de Cantabria, 39005 Santander, Spain

J. Garcia-Jaca

Departamento de Química Inorgánica, Facultad de Ciencias Químicas, Universidad Complutense de Madrid, 28040 Madrid, Spain

H. Ehrenberg and H. Weitzel

Fachgebiet Strukturforchung, Fachbereich Materialwissenschaft, Technische Universität, D-64287 Darmstadt, Germany

(Received 24 January 2000)

The aim of this work is to investigate the origin of the piezochromism and thermochromism exhibited by the copper oxide CuMoO_4 . These optical phenomena are associated with structural phase transition (PT) from the triclinic α (green) modification to the γ (brownish-red) modification. The variation of the optical-absorption spectrum with pressure and temperature indicates that the piezochromic and thermochromic transitions can be reached from ambient conditions either by applying pressure at 2.5 kbar or by cooling at $T=200$ K. We show that the change of color at the $\alpha \rightarrow \gamma$ PT is due to the broadening of the first $\text{O}^{2-} \rightarrow \text{Cu}^{2+}$ charge-transfer band, and the disappearance of an intense peak at 1.49 eV, related to the presence of pyramidal CuO_5 complexes in $\alpha\text{-CuMoO}_4$. The measured oscillator strength suggests that this peak corresponds to the $e \rightarrow b_1$ crystal-field transition within CuO_5 rather than to an $\text{O}^{2-} \rightarrow \text{Cu}^{2+}$ charge-transfer band. The correlation between optical and structural properties performed in this work confirms this interpretation, and also explains the strong dichroism exhibited by the crystal in the high-pressure $\gamma\text{-CuMoO}_4$ modification.

I. INTRODUCTION

CuMoO_4 is an interesting copper oxide, which exhibits piezochromic and thermochromic properties. Its p - T phase diagram has been recently determined in a wide range of pressure and temperature.¹ Among the four identified phases, the stable phase $\alpha\text{-CuMoO}_4$ at atmospheric pressure and room temperature transforms into the $\gamma\text{-CuMoO}_4$ phase either by applying pressure or by cooling. The crystal is triclinic ($P\bar{1}$ space group) in both α (green) and γ (brownish red) modifications, and the corresponding first-order $\alpha \rightarrow \gamma$ phase transition (PT) is accompanied by an intense green-to-brownish-red change of color. A salient feature of this material is the enormous volume reduction of 13% at this PT. This reduction correlates with an increase in the Cu-complex packing in $\gamma\text{-CuMoO}_4$. In fact, the phase transition involves a change in the copper coordination of $\frac{1}{3}$ Cu^{2+} ions from square-pyramidal (C_{4v}) CuO_5 in $\alpha\text{-CuMoO}_4$ to octahedral elongated (D_{4h}) CuO_6 in $\gamma\text{-CuMoO}_4$. The remaining $\frac{2}{3}$ Cu^{2+} displays an octahedral elongated coordination in both phases (Fig. 1). In the high-pressure or low-temperature $\gamma\text{-CuMoO}_4$ phase, however, all Cu^{2+} ions display an octahedral coordination CuO_6 with average Cu-O bond lengths: $R_{\text{ax}}=2.38$ Å and $R_{\text{eq}}=1.95$ Å. In $\alpha\text{-CuMoO}_4$, average Cu-O distances are $R_{\text{ax}}=2.37$ Å and $R_{\text{eq}}=1.96$ Å for octahedral coordinated CuO_6 , whereas they are $R_{\text{ax}}=2.34$ Å and $R_{\text{eq}}=1.93$ Å for pyramidal (C_{4v}) CuO_5 . Rather than bond-length modifications of O-Cu and Mo-O, the displacive $\alpha \rightarrow \gamma$ PT involves a rearrangement of the copper complexes, in such a way that terminal O^{2-} ligands of CuO_6 in $\alpha\text{-CuMoO}_4$ approach the pyramidal CuO_5 complexes leading to linked ligand-shared CuO_6 units in $\gamma\text{-CuMoO}_4$ (Fig.

1). The isolated six-Cu cluster structure in $\alpha\text{-CuMoO}_4$ becomes interconnected in $\gamma\text{-CuMoO}_4$, forming copper oxide layers spanned by $[1,1,1]$ and $[1, -5, 1]$ lattice vectors.¹

In this work we investigate the optical-absorption (OA) spectra of single crystals of CuMoO_4 , and their variations with pressure and temperature. Attention is paid to changes undergone by the OA spectra around the $\alpha \rightarrow \gamma$ structural PT, which is responsible for the piezochromism and thermochromism. The OA peak assignment is performed on the basis of the molecular-orbital diagrams within CuO_5 and CuO_6 complexes, by correlating the OA spectrum and the crystal structure in each phase. The electronic structure for CuO_5 and CuO_6 in $\gamma\text{-CuMoO}_4$ and $\alpha\text{-CuMoO}_4$ modifications has been calculated by means of extended-Hückel-type calculations. This information is useful to explore electronic structure variations associated with coordination changes of the complex: $\text{CuO}_5 \rightarrow \text{CuO}_6$.

II. EXPERIMENT

The green $\alpha\text{-CuMoO}_4$ was obtained at ambient pressure, as described elsewhere.^{2,3} The OA spectra under pressure were obtained by means of a single-beam microspectrometer,⁴ implemented for working with high absorbing materials. A platelike CuMoO_4 single crystal of $100 \times 60 \times 20$ μm^3 , with a quasitrapezoidal base oriented nearly perpendicular to the \mathbf{b} direction, was employed for pressure experiments in this research. The pressure was applied by means of a DAC (High Pressure Diamond Optics, Inc.), and calibrated from the Ruby R -line shift. The electronic energy-level diagram of CuO_5 and CuO_6 polyhedra were studied using extended Hückel calculations.⁵⁻⁷

The polarized OA spectra of single crystals as a function

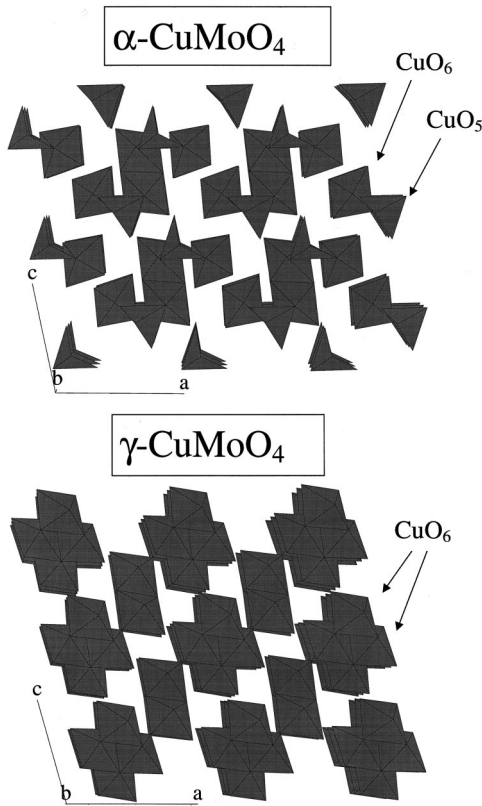


FIG. 1. Crystallographic structure of the α and γ phases of CuMoO_4 (triclinic, $P\bar{1}$ space group). For the sake of clarity we only show the CuO_6 and CuO_5 polyhedra. The lattice parameters are $a = 9.901 \text{ \AA}$, $b = 6.786 \text{ \AA}$, $c = 8.369 \text{ \AA}$, $\alpha = 101.13^\circ$, $\beta = 96.88^\circ$, and $\gamma = 107.01^\circ$ (α phase); and $a = 9.708 \text{ \AA}$, $b = 6.302 \text{ \AA}$, $c = 7.977 \text{ \AA}$, $\alpha = 94.76^\circ$, $\beta = 103.35^\circ$, and $\gamma = 103.26^\circ$ (γ phase).

of temperature were recorded with a Lambda 9 Perkin-Elmer spectrophotometer equipped with Glan-Taylor polarizing prisms, and operating with a fixed bandwidth of 1 nm. The sample thickness for the absorption was about 0.05 mm. The crystals were mounted on an OFHC (oxygen free high conductivity) copper plate over a 0.3-mm hole. A proper thermal contact was attained using crycon grease. Crystals were oriented with the light polarization along the extinction directions with a polarizing microscope. The temperature was varied in the 10–300 K range with a Scientific Instruments 202 closed-circuit cryostat and an APD-K controller, providing a temperature accuracy of 1 K.

III. RESULTS AND DISCUSSION

A. Absorption spectrum of CuMoO_4

Figure 1 shows the triclinic $P\bar{1}$ crystallographic structure of the α - CuMoO_4 and γ - CuMoO_4 phases viewed nearly along the $[010]$ direction. The corresponding OA spectra obtained from single crystals of CuMoO_4 are shown in Fig. 2. The spectrum for α - CuMoO_4 is nearly isotropic, and was obtained at zero pressure and $T = 295 \text{ K}$, whereas the OA spectrum for γ - CuMoO_4 was taken either at $P = 10 \text{ kbar}$ and room temperature, or below the phase transition temperature $T = 200 \text{ K}$ at zero pressure. The γ spectrum is strongly dependent on the light polarization, and its color

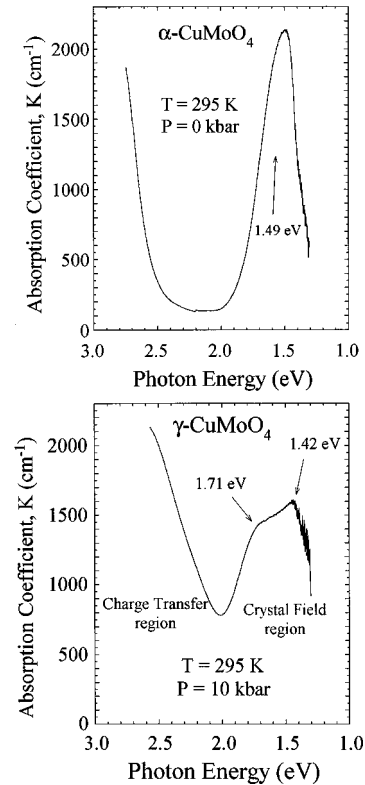


FIG. 2. Optical-absorption spectra at $T = 295 \text{ K}$ corresponding to a single crystal of CuMoO_4 at $P = 0$ (α phase), and at $P = 10 \text{ kbar}$ (γ phase). The latter spectrum is also obtained at $P = 0$ and $T < 150 \text{ K}$. The light is transmitted nearly parallel to the \mathbf{b} direction. Crystal dimensions $100 \times 60 \times 20 \text{ \mu m}^3$. The absorption coefficient is given by $K = 1/l \ln(I_0/I)$, where l is the sample thickness, and I_0 and I , represent the transmitted light intensity through the hydrostatic medium and the sample within the DAC, respectively.

changes from brownish red to dark brown when the light polarization is rotated from one extinction direction to another. The brownish red extinction is mainly associated with the axial elongation of the CuO_6 octahedra, while the perpendicular extinction is in the layers. Although the peak structures of spectra α and γ are independent of the polarization direction, the absorption background (AB) for γ - CuMoO_4 increases by about two optical density units depending on whether the polarization is nearly along the elongated axis of the CuO_6 octahedra or nearly the equatorial plane of the complex, respectively. The dark brown color is just associated with the increase of the AB. The corresponding OA spectrum could not be obtained due to high optical density values in this polarization.

B. Piezochromism and thermochromism

Figure 3 shows the variation of the OA spectra of a single crystal of CuMoO_4 as a function of pressure. The abrupt change undergone by the spectrum above 3 kbar reveals the $\alpha \rightarrow \gamma$ PT, and therefore the associated OA spectra taken below and above this critical pressure must correspond to α - CuMoO_4 and γ - CuMoO_4 , respectively. An analogous variation is also observed upon cooling the crystal in the 300–10 K temperature range. In this case, the OA spectrum

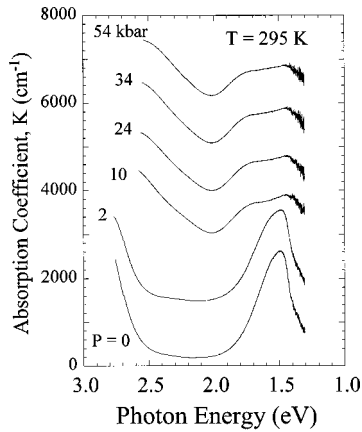


FIG. 3. Variation of the OA spectrum of CuMoO_4 with pressure in the 0–60-kbar range at $T=295$ K. Crystal dimensions $100 \times 60 \times 20 \mu\text{m}^3$. The pressure was determined through the R -line shift of the ruby luminescence. A constant absorption background has been added to each spectrum for comparison purposes.

abruptly changes at $T=200$ K, as it is clearly evidenced from Fig. 4. Figure 4 shows the variation of the crystal optical density at $\lambda = 540$ nm as a function of the temperature, and the inset shows the corresponding polarized OA spectra at $T=10$ K from a (001) platelike crystal. We selected this wavelength since the associated energy, $E=2.30$ eV, provides maximum variations of optical density at the $\alpha \rightarrow \gamma$ PT. The curve was taken in the cooling run at a rate of 1 K/min. The observed variation clearly indicates that the thermochemical transition temperature is $T_C=200$ K. A precise value of the thermal hysteresis associated with the $\alpha \rightarrow \gamma$ first-order phase transition could not be properly measured due to crystal cracking below T_C . However, a thermal

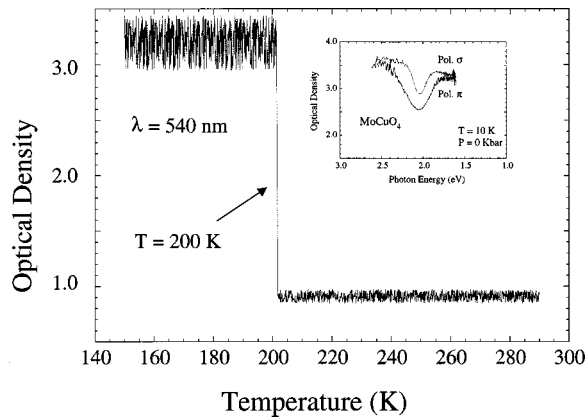


FIG. 4. Temperature dependence of the crystal optical density at $\lambda = 540$ nm ($E = 2.30$ eV). The abrupt jump at $T_C = 200$ K indicates the thermochemical PT of CuMoO_4 at $P = 0$. The curve was obtained in the cooling run at a fixed wavelength. Cooling rate: 1 K/min. In the corresponding heating run three jumps at $T = 220$, 247, and 250 K (not shown here) have been observed. The jumps are associated with the occurrence of the $\gamma \rightarrow \alpha$ PT in different crystal regions, which were probably isolated due to crack formation during the cooling run. The inset shows the polarized OA spectrum corresponding to a (001) platelike crystal at $T = 10$ K. The polarizations correspond to the two extinction directions, with the σ polarization close to the crystal layers. Optical densities above 3 could not be properly measured in $\gamma\text{-CuMoO}_4$.

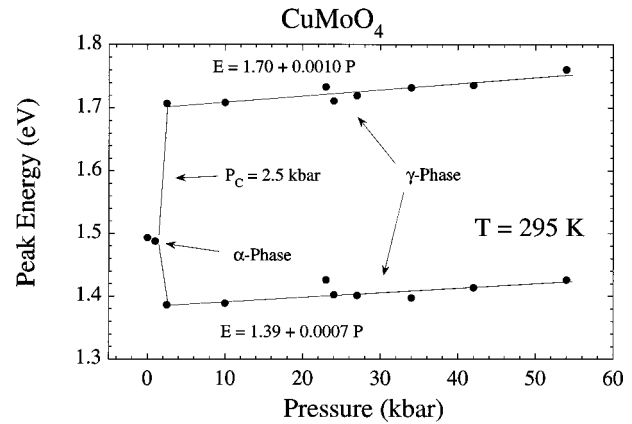


FIG. 5. Variation of the CF peak energy with pressure in CuMoO_4 . Note the abrupt change undergone by the peak energy at the piezochromic PT, $P_C = 2.5$ kbar.

hysteresis of $\Delta T = T_{C\text{-Heating}} - T_{C\text{-Cooling}} = 20\text{--}30$ K, could be estimated from the heating run, taking the temperature at which the first optical density jump occurs as PT temperature ($T_{C\text{-Heating}}$). Due to crystal cracks, there are crystal regions with deficient thermal contact, thus undergoing the PT at slightly different temperatures. The three optical density jumps observed in the heating-run curve at $T = 220$, 247, and 250 K are probably related to the occurrence of the $\gamma \rightarrow \alpha$ PT in different crystal domains.

The OA spectra corresponding to $\alpha\text{-CuMoO}_4$ and $\gamma\text{-CuMoO}_4$ (Figs. 2 and 3) indicate that the piezochromism or thermochemical accompanying the PT can be described by changes in the crystal transmittance. The green color of the α phase actually corresponds to the optical window between 2 eV (600 nm) and 2.5 eV (500 nm), formed by the tails of two absorption peaks placed at 1.49 eV and around 3 eV. On the other hand, the brownish red color of the γ modification is due to the narrowing and redshift of the optical window, whose transmittance maximum is displaced to 2 eV (600 nm). In terms of absorption bands, the red color is produced by the broadening of the UV band and the disappearance of the 1.49-eV absorption peak, both effects favoring a shift of the transmittance maximum to the red. In addition this broadening is also responsible for the increase of the AB on passing from $\alpha\text{-CuMoO}_4$ ($K_{AB} = 100 \text{ cm}^{-1}$) to $\gamma\text{-CuMoO}_4$ ($K_{AB} = 800 \text{ cm}^{-1}$), as shown in the OA spectra of Fig. 2. The peak energy variation around 1.5 eV with pressure is depicted in Fig. 5. The peak energies have been obtained through suitable programs for spectrum analysis using two Gaussian bands to describe the OA spectrum around 1.5 eV. The results clearly reveal the occurrence of the piezochromic PT at $P_C = 2.5$ kbar. Furthermore, the small energy shifts observed in each phase (~ 1 meV/kbar) reflect the weak sensitivity of the OA peaks to pressure. The presence of two components at 1.39 and 1.71 eV in the high-pressure phase should not be related to the splitting of the 1.49-eV peak, but to the disappearance of this peak at the PT, and the occurrence of two new peaks in the $\gamma\text{-CuMoO}_4$ spectrum.

C. Peak assignment and dichroism in $\alpha\text{-CuMoO}_4$ and $\gamma\text{-CuMoO}_4$

The OA spectrum shown in Fig. 2 basically consists of two peaks around 3 and 1.49 eV, which are characteristics of

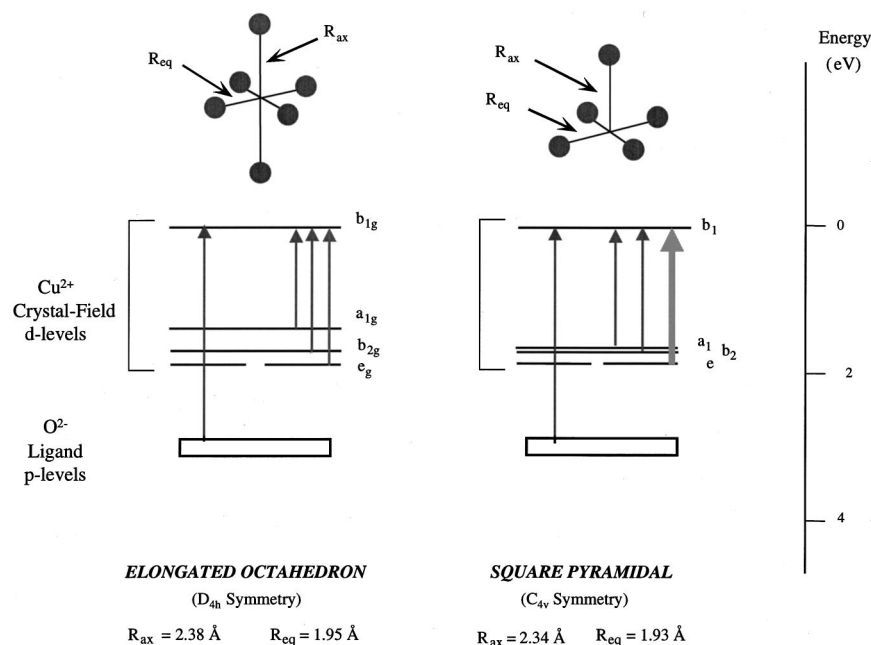


FIG. 6. One-electron energy-level diagram for CuO_5 and CuO_6 complexes obtained from extended Hückel calculations. The thick arrow indicates the symmetry-allowed electric-dipole CF transition $e \rightarrow b_1$ in CuO_5 . The other arrows on the right side of the diagram show the assisted CF transitions, and the left side arrows represent the first allowed CT transitions. The energies have been calculated using the Cu-O bond distances obtained from x-ray diffraction (Ref. 1).

$\text{O}^{2-} \rightarrow \text{Cu}^{2+}$ charge transfer (CT) transitions and crystal-field (CF) Cu^{2+} d - d transitions respectively.^{8–10} The extended-Hückel calculations performed for CuO_5 and CuO_6 complexes confirm this interpretation (Fig. 6). We only observe the low-energy tail of the CT band in the OA spectrum, due to the high oscillator strength of the $e_u \rightarrow b_{1g}(x^2-y^2)$ ligand to metal CT transition ($f_{\text{OS}} \sim 0.1-0.01$) compared to the CF ones ($f_{\text{OS}} \sim 10^{-4}$).⁸ In γ - CuMoO_4 , where all Cu^{2+} ions display an elongated octahedral coordination (CuO_6), the two components at 1.39 and 1.71 eV correspond to CF transitions from the t_{2g} parent octahedral, mainly $\text{Cu}^{2+} e_g(xz, yz)$ and $b_{2g}(xy)$ molecular orbitals (MO's) to the half-filled $b_{1g}(x^2-y^2)$ MO's within a CuO_6 (D_{4h}) complex (Fig. 6). The CF transitions are weaker than the corresponding $e_u \rightarrow b_{1g}$ CT ones, since they involve MO's of the same parity. However, CF transitions can gain intensity through the electric dipole mechanism by noncentrosymmetric ligand field distortions of the complex induced either by crystal anisotropy, by coupling to odd symmetry vibrations, or by the exchange mechanism in concentrated materials. In the vibrational mechanism, the enhancement of intensity is thermally activated. The measured oscillator strength for these two CF transitions are $f_{\text{OS}} = 7 \times 10^{-5}$, which are characteristic of CF transitions in 3d-metal (transition metal) complexes.^{8,9}

Interestingly, the correlation between the crystal structure of the α and γ phases and their OA spectrum (Fig. 2) indicates that the intense peak at 1.49 eV is related to CuO_5 , since it does not appear in γ - CuMoO_4 , where all Cu^{2+} are hexacoordinated CuO_6 . This conclusion is in agreement with findings in the semiconducting green compounds Y_2BaCuO_5 and $\text{YBa}_2\text{Cu}_3\text{O}_6$,^{12,13} and the superconducting $\text{YBa}_2\text{Cu}_3\text{O}_x$ ($x=6-7$) series,^{10,11} whose absorption spectra, associated with pentacoordinated Cu^{2+} complexes, show a similar peak at 1.5 eV. Nevertheless there was some controversy on the assignment of this peak to a CF transition^{11,12} or to an $\text{O}^{2-} \rightarrow \text{Cu}^{2+}$ CT transition in CuO_5 .¹⁰ With the present results we assign this peak to the $e \rightarrow b_1$ CF transition. This assignment

is also supported by the measured oscillator strength, $f_{\text{OS}} = 8 \times 10^{-4}$, and the electronic structure calculations performed for CuO_5 and CuO_6 using the bond distances obtained from x-ray data:¹ $R_{\text{ax}} = 2.34 \text{ \AA}$ and $R_{\text{eq}} = 1.93 \text{ \AA}$ for CuO_5 , and $R_{\text{ax}} = 2.38 \text{ \AA}$ and $R_{\text{eq}} = 1.95 \text{ \AA}$ for CuO_6 . It must be noted that although these calculations do not give precise values of the transition energies, they provide a useful method to estimate roughly peak energy variations due to structural changes of the complex. From these calculations we conclude that the electronic structures for CuO_5 and CuO_6 are very similar (Fig. 6). We obtain CF transition energies of 1.87 eV for $e \rightarrow b_1$ in CuO_5 , and 1.87, 1.71, and 1.40 eV for $e_g \rightarrow b_{1g}$, $b_{2g} \rightarrow b_{1g}$, and $a_{1g} \rightarrow b_{1g}$ in CuO_6 , respectively, whereas the corresponding first $e \rightarrow b_1$ and $e_u \rightarrow b_{1g}$ CT transitions are calculated at 3 eV in both complexes. It is worth noting that the first symmetry-allowed CT energy does not change significantly upon a change of Cu^{2+} coordination for CuO_5 to CuO_6 ; hence we ascribe the 1.49-eV peak observed in α - CuMoO_4 to the $e \rightarrow b_1$ CF transition in CuO_5 rather than to a ligand-to-metal CT transition. Moreover the oscillator strength measured for the 1.49-eV peak, $f_{\text{OS}} = 8 \times 10^{-4}$, is about two orders of magnitude weaker than the CT values,^{8,14} thus making the assignment to a CT transition unlikely. On the other hand, f_{OS} is somewhat higher than the oscillator strength measured for the other two CF peaks in γ - CuMoO_4 ($f_{\text{OS}} = 7 \times 10^{-5}$), as well as for other d - d transitions.^{8,9} The intensity enhancement of the 1.49-eV CF peak in CuO_5 with respect to CuO_6 is presumably due to the noncentrosymmetric character of the CuO_5 complex (C_{4v}). Actually, $e \rightarrow b_1$ is the only symmetry-allowed CF transition in C_{4v} , and therefore must be a major feature of the CF spectrum in α - CuMoO_4 . This fact explains why the CF spectrum at ambient pressure is dominated by CuO_5 , and the presence of the two CF peaks associated with the remaining $\frac{2}{3}$ CuO_6 are masked by this peak. The coordination change $\text{CuO}_5 \rightarrow \text{CuO}_6$ at the $\alpha \rightarrow \gamma$ PT leads to the disappearance of this peak, making the two peaks at 1.39 and 1.71 eV visible in the γ - CuMoO_4 spectrum.

The CT band broadening observed at the PT is noteworthy. It plays a key role in the piezochromic and thermochromic properties of this material. This CT broadening is presumably related to the compactness of the copper complexes in the high-pressure phase. This effect is probably a consequence of the larger overlap between the p -oxygen orbitals forming the valence band in γ -CuMoO₄. In contrast to α -CuMoO₄, Cu²⁺ ions in the high-pressure brownish red phase are no longer isolated in six-copper clusters, but form layers perpendicular to $[7, 1, -11]$,¹ with the elongated axis of all CuO₆ complexes oriented along the same crystallographic direction (Fig. 1). This preferential orientation is important to understand the strong dichroism exhibited by single crystals of γ -CuMoO₄. Either a brownish red color or a very dark brown crystal is observed depending on whether the light polarization is nearly parallel to the octahedral elongation or is close to the equatorial plane of the complex, respectively. This effect has a great influence on the AB and hence on the crystal color, given that the $e_u \rightarrow b_{1g}$ CT band is completely polarized in the equatorial plane of the complex.

IV. CONCLUSIONS

In this work it is shown that the piezochromism and thermochromism of CuMoO₄ is associated with the occurrence

of the $\alpha \rightarrow \gamma$ PT either at $P=2.5$ kbar and $T=295$ K or at $P=0$ and $T=200$ K. The variation observed in the OA spectrum at the PT is related to coordination changes from CuO₅ \rightarrow CuO₆ in $\frac{1}{3}$ Cu²⁺ ions. The color change from green to brownish red is due to the disappearance of the 1.49-eV peak and the broadening of the CT band at 3 eV. This effect correlates with the structural change undergone by the crystal on passing from α -CuMoO₄ to γ -CuMoO₄, leading to an increase of the AB and a redshift of the maximum transmittance. The strong dichroism observed in γ -CuMoO₄ is explained by the formation of copper oxide layers in this phase. This work also clarifies the origin of the 1.49 peak as the $e \rightarrow b_1$ CF transition in CuO₅, and rules out the possibility as a CT transition within CuO₅. In fact, the first O²⁻ \rightarrow Cu²⁺ CT energy in CuO₅ is similar to the first CT band in CuO₆, according to the OA spectra of both α and γ phases and extended Hückel calculations.

ACKNOWLEDGMENTS

This work was supported by Caja Cantabria, The Vicerectorado de Investigación of the University of Cantabria and the CICYT (Project No. PB98-0190).

*Corresponding author.

Electronic address: rodriguf@ccaix3.unican.es

¹M. Wiesmann, H. Ehrenberg, G. Miehe, T. Peun, H. Weitzel, and H. Fuess, *J. Solid State Chem.* **132**, 88 (1997).

²H. Ehrenberg, G. Wltschek, F. Trouw, T. Kroener, H. Weitzel, and H. Fuess, *J. Magn. Magn. Mater.* **135**, 355 (1994).

³H. Ehrenberg, H. Weitzel, H. Paulus, M. Wiesmann, G. Wltschek, M. Geselle, and H. Fuess, *J. Phys. Chem. Solids* **58**, 153 (1997).

⁴B. A. Moral and F. Rodríguez, *Rev. Sci. Instrum.* **66**, 5178 (1995); D. Hernández, Ph.D. thesis, University of Cantabria, 1998.

⁵R. Hoffmann and W. N. Lipscomb, *J. Chem. Phys.* **36**, 2179 (1962).

⁶R. Hoffmann, *J. Chem. Phys.* **39**, 1397 (1963).

⁷M. H. Whangbo, M. Evain, T. Hungbanks, M. Kertesz, S. D. Wijeyesekera, C. Wilker, Z. Zheng, and R. Hoffman, *Quantum*

Chemistry Program Exchange No. 571, 1978.

⁸A. B. P. Lever, *Inorganic Electronic Spectroscopy Studies in Physical and Theoretical Chemistry* (Elsevier, New York, 1984).

⁹F. Rodríguez, P. Núñez, and M. C. Marco de Lucas, *J. Solid State Chem.* **110**, 370 (1994).

¹⁰J. M. Leng, J. M. Ginder, W. E. Farneth, S. I. Shah, and E. J. Epstein, *Phys. Rev. B* **43**, 10 582 (1988).

¹¹M. K. Kelly, P. Barboux, J. M. Tarascon, D. E. Aspnes, W. A. Bonner, and P. A. Morris, *Phys. Rev. B* **38**, 870 (1988).

¹²P. Adler and A. Simon, *Z. Phys. B: Condens. Matter* **85**, 197 (1991).

¹³T. Yamamoto, K. Shinagawa, T. Saito, and T. Tsushima, *Jpn. J. Appl. Phys.* **31**, L327 (1992).

¹⁴R. Valiente and F. Rodríguez, *J. Phys. Chem. Solids* **57**, 571 (1996).